



Contents lists available at ScienceDirect

Continental Shelf Research

journal homepage: www.elsevier.com/locate/csr

Modeling the response of primary production and sedimentation to variable nitrate loading in the Mississippi River plume

Rebecca E. Green^{a,*}, Greg A. Breed^b, Michael J. Dagg^{c,1}, Steven E. Lohrenz^{d,2}

^a Ocean Sciences Division, Naval Research Laboratory, Stennis Space Center, MS 39529, USA

^b Department of Biology, Dalhousie University, Halifax, NS, Canada B3H 4J1

^c Louisiana Universities Marine Consortium, Chauvin, LA 70344, USA

^d Department of Marine Science, University of Southern Mississippi, Stennis Space Center, MS 39529, USA

ARTICLE INFO

Article history:

Received 21 May 2006

Received in revised form

13 November 2006

Accepted 15 February 2007

Available online 6 March 2008

Keywords:

Ecosystem model

Mississippi River plume

Nitrogen

Primary production

Sedimentation

ABSTRACT

Increases in nitrate loading to the Mississippi River watershed during the last 50 years are considered responsible for the increase in hypoxic zone size in Louisiana-Texas shelf bottom waters. There is currently a national mandate to decrease the size of the hypoxic zone to 5000 km² by 2015, mostly by a 30% reduction in annual nitrogen discharge into the Gulf of Mexico. We developed an ecosystem model for the Mississippi River plume to investigate the response of organic matter production and sedimentation to variable nitrate loading. The nitrogen-based model consisted of nine compartments (nitrate, ammonium, labile dissolved organic nitrogen, bacteria, small phytoplankton, diatoms, micro- and mesozooplankton, and detritus), and was developed for the spring season, when sedimentation of organic matter from plume surface waters is considered important in the development of shelf hypoxia. The model was forced by physical parameters specified along the river-ocean salinity gradient, including residence time, light attenuation by dissolved and particulate matter, mixed layer depth, and dilution. The model was developed using measurements of biological biomasses and nutrient concentrations across the salinity gradient, and model validation was performed with an independent dataset of primary production measurements for different riverine NO₃ loads. Based on simulations over the range of observed springtime NO₃ loads, small phytoplankton contributed on average 80% to primary production for intermediate to high salinities (>15), and the main contributors to modeled sedimentation at these salinities were diatom sinking, microzooplankton egestion, and small phytoplankton mortality. We investigated the impact of limiting factors on the relationship between NO₃ loading and ecosystem rates. Model results showed that primary production was primarily limited by physical dilution of NO₃, followed by abiotic light attenuation, light attenuation due to mixing, and diatom sinking. Sedimentation was mainly limited by the first three of these factors. Neither zooplankton grazing or plume residence times acted as limiting factors of ecosystem rates. Regarding nutrient reductions to the watershed, simulations showed that about half of the percent decrease in NO₃ load was reflected in decreased plume sedimentation. For example, a 30% decrease in NO₃ load resulted in a 19% decrease in average plume primary production and a 14% decrease in sedimentation. Finally, our model results indicated that the fraction of primary production exported from surface waters is highly variable with salinity (7–87%), a finding which has important implications for predictive models of hypoxic zone size that assume a constant value for this ratio.

© 2008 Elsevier Ltd. All rights reserved.

1. Introduction

The Mississippi River delivers high concentrations of inorganic nutrients to coastal waters of the northern Gulf of Mexico, currently the second largest zone of coastal hypoxia in the world (Rabalais et al., 2002). Hypoxic bottom waters (dissolved oxygen concentrations <2 mg L⁻¹) are a concern primarily because of the lack of catchable demersal fish, shrimp, and crabs in these waters (Leming and Stuntz, 1984). It is conventionally understood that a fraction of production sinks from surface waters to below a

* Corresponding author. Tel.: +1 228 688 5576; fax: +1 228 688 4149.

E-mail addresses: rgreen@nrlssc.navy.mil (R.E. Green), gbreed@dal.ca (G.A. Breed), mdagg@lumcon.edu (M.J. Dagg), steven.lohrenz@usm.edu (S.E. Lohrenz).

¹ Tel.: +1 985 851 2856; fax: +1 985 851 2874.

² Tel.: +1 228 688 3177; fax: +1 228 688 1121.

pycnocline—a barrier for oxygen exchange with the atmosphere—where it is consumed by aerobic bacteria leading to hypoxic conditions in bottom waters. However, the linkage between nutrient delivery to surface waters and organic matter sedimentation to bottom waters is complex due to the interplay of numerous physical and biological factors controlling vertical flux. In the 1990s, several observational research programs endeavored to better understand the oceanographic processes controlling organic sedimentation and ecosystem variability on the Louisiana–Texas (LATEX) shelves. These programs produced a suite of ecosystem data, and the first ecosystem-scale attempt to quantify how primary productivity and sedimentation were linked. Factors regulating phytoplankton biomass and primary production near the Mississippi River delta include riverine nutrient flux, low irradiance in low salinity waters, nutrient limitation at high salinities, mixing and advection, and grazing (e.g., Lohrenz et al., 1990, 1999; Dagg, 1995). The fraction of production exported from the euphotic zone was observed to vary widely on the Louisiana Shelf, dependent in part on phytoplankton species composition and on the grazing activities of microzooplankton and mesozooplankton (Redalje et al., 1994).

Numerical models have been developed for predicting the areal extent of hypoxia formation on the LATEX shelf, as a function of nutrient loading. Three models were used to predict inter-annual variations in hypoxic zone size and resulted in suggestions for the regulation of nutrient inputs to the Mississippi River, including a two-box, oxygen flux model (Justić et al., 2002) and three-dimensional (Bierman et al., 1994) and one-dimensional mass balance models (Scavia et al., 2003, 2004). Management plans for reducing the size of regional hypoxia involve reducing nitrogen inputs to the Mississippi River watershed by a certain percentage. A task force convened to recommend policy actions and forwarded to the US Congress in 2002 the suggestion that nitrogen inputs to the watershed be reduced by 30% (Rabalais et al., 2002). Based on their model results, Scavia et al. (2004) proposed that this percentage be increased to 40% if the goal of decreasing the areal extent of the hypoxic zone by two-thirds is to be achieved. Though these models roughly succeed at predicting hypoxic zone size based on nutrient inputs, they provide little mechanistic understanding of the relationship between surface water food web processes in the plume and how these processes change under variable riverine nutrient loadings. For example, several of the models assume that a constant 50% of primary production is exported vertically (Scavia et al., 2003; Justić et al., 1997; Rabalais et al., 1991). This assumption has important implications, because the measured export ratio is known to vary greatly both spatially and temporally on the Louisiana shelf due to changes in physical and biological forcing (Redalje et al., 1994).

The development of food web models to describe organic matter cycling on the Louisiana shelf is still in its infancy. Recently, an inverse food web model was developed and employed for the Mississippi River plume (MRP) to better understand ecosystem dynamics and organic carbon flows between bacteria, small and large phytoplankton, protozoans, microzooplankton, mesozooplankton, dissolved organic carbon (DOC), and detritus (Breed et al., 2004). This model helped illuminate spatial and temporal variability in the relationship between primary productivity and vertical export. It was also used to construct an organic carbon budget for the Mississippi River turbidity plume and to calculate plume contributions to the development of shelf hypoxia (Green et al., 2006). The inverse analysis technique used in the food web model is only applicable to hindcasting, and hence there is a clear need for a predictive food web model that can forecast ecosystem response to variable nitrate loading. Such a nitrogen-based model of planktonic dynamics was originally presented by Fasham et al. (1990). Their

nitrogen–phytoplankton–zooplankton (NPZ) model was used to describe the annual cycle of planktonic dynamics and nitrogen cycling in the oceanic mixed layer near Bermuda. Following modification for more eutrophic waters, variations of their model have since been applied in more coastal regimes (e.g., Huret et al., 2005). The NPZ model accounts for nutrient and light limitation, computes flows between living (bacteria, phytoplankton, and zooplankton) and non-living (detrital) compartments, and assigns detrital sinking rates for the computation of organic matter sedimentation.

Our goal was to model the relationship between riverine NO_3 loading and ecosystem processes in surface waters of the MRP. There is currently little understanding of the relationship between NO_3 loading and organic matter sedimentation from the river plume, and our intention was to develop a predictive model to better quantify this relationship. We developed a nine-compartment ecosystem model to simulate planktonic dynamics and response to variable nitrate loading in the buoyant surface plume. The original Fasham et al. (1990) NPZ model was modified to include more biological compartments (two groups each for phytoplankton and zooplankton) and to describe processes along a salinity transect of the plume during the spring season. Physical and biological components of the ecosystem model were developed based on previous observational studies in the MRP. Our model was developed by comparison of model results and measurements across the salinity gradient, and the model was validated through comparison with independent measurements of primary production for different nitrate loads. We then applied the model to answering our main question: How do changes in riverine nitrate inputs affect food web structure and sedimentation of particulate organic nitrogen (PON) from the surface plume? We also determined the primary factors limiting the effect of riverine nitrogen loading on primary production, phytoplankton community structure, and sedimentation.

2. Methods

We constructed a nine-compartment coupled differential equation model to simulate biological and chemical dynamics in the MRP. The model included a number of simple physical dynamics which were constrained by field data (Fig. 1). Whereas time is often an annual cycle in an NPZ model (Fasham et al., 1990), we defined time as transport through the river plume from the river mouth to the high salinity plume edge; this is a zero-D, lagrangian model in which time is equivalent to moving across the salinity gradient when the plume is in steady state. Physical and biological processes were modeled to represent average spring-time conditions, a season during which primary production in LATEX shelf surface waters is considered important to hypoxia development.

2.1. Physical model

The ecosystem model was forced by a simple physical model which included plume residence times and parameterizations of the abiotic in-water light field. Previous estimates of plume residence times were made by Breed et al. (2004) based on flow velocities in the plume determined from drifter data. They calculated residence times in three plume salinity sub-regions of 1 day in sub-region 1 (salinity 0–18), 1.5 days in sub-region 2 (18–27), and 6 days in sub-region 3 (27–32). We have adopted these values, in addition to assuming a residence time of 6 days for the highest salinity sub-region (32–36), equal to the residence time for sub-region 3. We modeled the relationship between transit time and salinity using these residence times and a

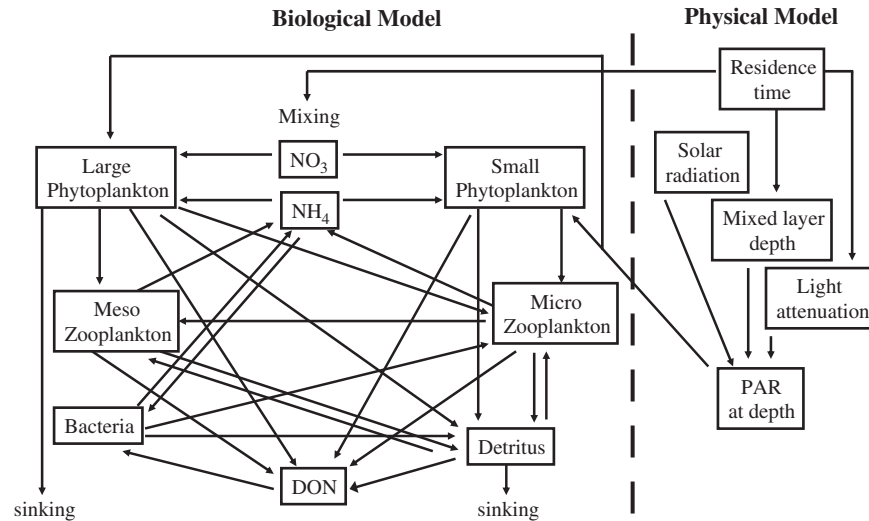


Fig. 1. Inter-compartmental flow chart of linkages between biological and physical ecosystem processes. Flows in the biological model are in units of $\mu\text{MN m}^{-3}$.

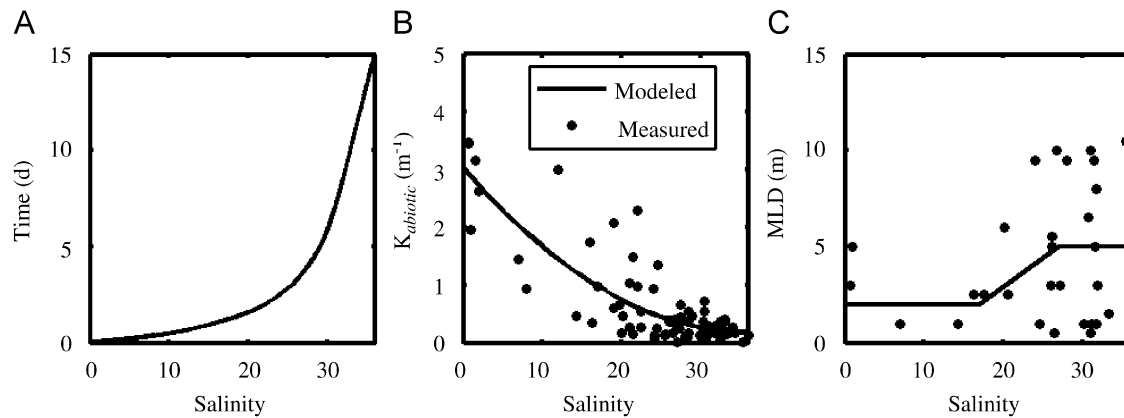


Fig. 2. Physical model parameterizations of salinity versus (A) residence time, (B) abiotic light attenuation (by CDOM and non-chlorophyllous SPM), and (C) mixed layer depth, based on comparison to measured values. These are the physical values that were used to force the model. Plume transit times were estimated from Breed et al. (2004).

sigmoidal function (Fig. 2(A)). The resulting relationship between time and salinity was

$$\text{salinity} = a_1 \times \frac{a_2 - a_3 \times e^{-a_4/t}}{a_5 - a_6 \times e^{-a_7/t}}, \quad (1)$$

where a_1 – a_7 are coefficients that were optimized to best fit estimated residence times, with values of $a_1 = 1.178$, $a_2 = 6.757 \times 10^{-6}$, $a_3 = -9.49 \times 10^{-6}$, $a_4 = 45.4$, $a_5 = 1.3729200894$, $a_6 = -1.3729198727$, and $a_7 = 2.084 \times 10^{-7}$ (for each coefficient, these were the minimum number of significant figures needed to reproduce the relationship). Measured transects of NO_3 along the plume have shown the importance of conservative mixing in controlling NO_3 concentrations (e.g., Lohrenz et al., 1999). Nitrate dilution in the model was calculated using two end-member mixing, with zero nitrate concentration at the high salinity end-member as

$$\text{dil} = 1 - \text{sal}/36. \quad (2)$$

The equation used in the model for dilution as a function of time is then calculated by substituting Eq. (1) into Eq. (2). We assumed that diffusion of NO_3 into surface waters from below the mixed layer was negligible. We did not include dilution effects on either NH_4 or dissolved organic nitrogen (DON), because biological activity seems to play the predominant role in controlling their concentrations in the plume (Pakulski et al., 2000).

Photosynthetically active radiation (PAR) in the water column was calculated from incident solar radiation, mixed layer depths (MLDs), and diffuse attenuation by optically active components in the water. Average daily incident solar radiation was calculated from the latitude (28.9°N), time of year (May 1), daylength, cloud cover (five oktas; J. Yuan, personal communication), solar constant (1368 W m^{-2}), and solar declination and zenith angle. Constant factors were used for the ratio of PAR to total irradiance (0.43; Jerlov, 1976) and the transmittance of light through the water surface (0.96; Gordon et al., 1988). Light is attenuated in the water column by phytoplankton, colored dissolved organic matter (CDOM), and suspended particulate matter (SPM). Attenuation due to phytoplankton is a dynamic term in the biological model, based on the concentration of phytoplankton and a cell self-shading term (Table 1). Our physical model included a parameterization of light attenuation by abiotic (non-chlorophyllous) material, which contributes to high light attenuation in low salinity plume waters. We used the model of Lohrenz et al. (1999) to calculate K_{abiotic} from springtime measurements of SPM, as follows:

$$K_{\text{abiotic}} = \frac{k_s \times \text{SPM}}{\mu_d}, \quad (3)$$

where k_s is the specific extinction coefficient for SPM ($0.03 \text{ m}^{-1} (\text{mg L}^{-1})^{-1}$) and μ_d is the average cosine of solar zenith angle over

Table 1
Model parameters

Parameter	Symbol	Value	Unit	Source
Light attenuation by phyto	K_{ph}	0.03	$m^{-1} (mmol m^{-3})^{-1}$	Huret et al. (2005)
Initial slope of $P-I$ curve	α	0.15	$d^{-1} (W m^{-2})^{-1}$	This study ^a
Max specific growth rate, $P1$	$\mu_{P1,max}$	3.12	d^{-1}	This study ^a
Max specific growth rate, $P2$	$\mu_{P2,max}$	3.36	d^{-1}	This study ^a
Phyto. specific mortality rate	m_p	0.03	d^{-1}	Huret et al. (2005)
NO_3 half-saturation, $P1$	$K_{NO_3,P1}$	0.2	$mmol m^{-3}$	Walsh et al. (2001)
NO_3 half-saturation, $P2$	$K_{NO_3,P2}$	1.7	$mmol m^{-3}$	Walsh et al. (2001)
NH_4 half-saturation, $P1$	$K_{NH_4,P1}$	0.1	$mmol m^{-3}$	Walsh et al. (2001)
NH_4 half-saturation, $P2$	$K_{NH_4,P2}$	2.0	$mmol m^{-3}$	Walsh et al. (2001)
Phyto. exudation fraction as DON	γ	0.05		Fasham et al. (1990)
Max grazing rate, $Z1$ on $P1, B, D$	$g_{Z1a,max}$	2.17	d^{-1}	This study ^a
Max grazing rate, $Z1$ on $P2$	$g_{Z1b,max}$	1.26	d^{-1}	This study ^a
Max grazing rate, $Z2$	$g_{Z2,max}$	1.5	d^{-1}	This study ^b
Zoopl. half-sat. for ingestion	K_g	1.0	$mmol m^{-3}$	Fasham et al. (1990)
Excretion, $Z1$	reg_{Z1}	1.2	d^{-1}	This study ^b
Excretion, $Z2$	reg_{Z2}	0.20	d^{-1}	This study ^b
Excretion, B	reg_B	0.50	d^{-1}	This study ^b
Fraction of Z excretion as NH_4	ϵ	0.77		Anderson and Williams (1998)
Fraction of Z mortality exported	Ω	0.125		Anderson and Williams (1998)
Specific mortality rate, $Z1$	m_{Z1}	0.3	$(mmol m^3 d)^{-1}$	This study ^b
Specific mortality rate, $Z2$	m_{Z2}	0.1	$(mmol m^3 d)^{-1}$	This study ^b
Assimilation efficiency, $Z1$ and $Z2$	β	0.75		Fasham et al. (1990)
Preference of $Z1$ for $P1, B,$ and D	p_1, p_2, p_3	0.7, 0.2, 0.1		Chai et al. (2002); This study
Preference of $Z2$ for $Z1, P2,$ and D				
Specific mortality rate, B	m_B	0.04	d^{-1}	Anderson and Williams (1998)
Detrital breakdown to DON	m_D	0.05	d^{-1}	Fasham et al. (1990)
Detrital sinking speed	v_D	5	$m d^{-1}$	Huret et al. (2005)
Diatom sinking speed	v_{P2}	1	$m d^{-1}$	Kelly-Gerrey et al. (2004)

^a Measured in the plume.

^b Chosen based on fit between modeled and measured values.

the daylight period (0.55). The impacts of CDOM are roughly included in this parameterization, because CDOM has been shown to co-vary with SPM in the plume (Lohrenz et al., 1999). The relationship between $K_{abiotic}$ and salinity was modeled using a second order polynomial which best fit the measured data ($K_{abiotic} = 2.20 \times 10^{-3}S^2 - 1.58 \times 10^{-1}S + 3.03$, where $K_{abiotic}$ is in units of m^{-1} and S is salinity; Fig. 2(B)). Additionally, light limitation of phytoplankton in the model was forced by MLDs throughout the plume. We estimated MLDs from springtime measurements (Lohrenz et al., 1999) as 2 m at low salinities increasing to 5 m at intermediate to high salinities (Fig. 2(C)).

2.2. Biological model

The biological model included the five living compartments of bacteria (B), small phytoplankton ($P1$), large phytoplankton (diatoms; $P2$), microzooplankton ($Z1$), and mesozooplankton ($Z2$), and the four non-living compartments of detrital nitrogen (DN), nitrate (NO_3), ammonium (NH_4), and labile DON . The inter-compartmental flows are shown schematically in Fig. 1; flows in the biological model are in units of $\mu M-N m^{-3}$. The non-diatom phytoplanktonic group covers all non-siliceous forms including cyanobacteria, flagellates, and dinoflagellates, although in the plume *Synechococcus* are likely the dominant group (e.g., Wawrik and Paul, 2004). The detrital compartment consists of fecal materials, dead phytoplankton, and dead zooplankton, and sinks at a set rate ($v_D = 5 m d^{-1}$; Table 1); the sum of sinking detritus and sinking diatoms determines the modeled sedimentation of organic matter to bottom waters. Biological concentrations are assumed to be homogenous within the mixed layer, such that the physical mixing rate is fast compared to the growth rates of organisms, and there is no diffusive mixing with waters below the mixed layer.

Large and small phytoplankton differed in their maximum growth rates and in their ability to compete for NO_3 and NH_4 , based on different Michaelis-Menten constants for nutrient uptake. Phytoplankton growth rate (σ) was modeled as a function of both light and nutrient limitation of cell growth, as represented by

$$\sigma = \mu_{max} \times \min(J, Q), \quad (4)$$

where J and Q are non-dimensional terms that determine light and nutrient limitation, respectively. Small and large phytoplankton growth rates (σ_{P1} and σ_{P2}) were defined by J and Q terms that were distinct for each phytoplankton group. The equation for J is the same as in Fasham et al. (1990). The nutrient limitation factor as a function of NO_3 and NH_4 was parameterized using an expanded Monod equation as follows:

$$Q = \frac{NO_3}{K_{NO_3} \left(1 + \frac{NO_3}{K_{NO_3}} + \frac{NH_4}{K_{NH_4}} \right)} + \frac{NH_4}{K_{NH_4} \left(1 + \frac{NO_3}{K_{NO_3}} + \frac{NH_4}{K_{NH_4}} \right)}, \quad (5)$$

where, as with the light limitation term, Q is separately defined for both small and large phytoplankton. The grazer compartments were differentiated by the type of potential prey, half-saturation constants and maximum grazing rates, and grazer preferences dependent on the type of prey item. The $P1$ phytoplankton class is quickly grazed by microzooplankton, whose grazing rate nears that of the small phytoplankton growth rate. The $P2$ phytoplankton class are consumed both by micro- and mesozooplankton ($Z1$ and $Z2$), and at a slower rate than $Z1$ feeds on $P1$. In addition to phytoplankton, both $Z1$ and $Z2$ graze on DN , $Z1$ grazes on bacteria, and $Z2$ grazes on $Z1$. Grazing rates were defined using

Table 2

Differential equations describing model flows

$$\begin{aligned} \frac{dP1}{dt} &= [(1 - \gamma)\sigma_{P1} - m_P]P1 - G_{Z1,P1}Z1 \\ \frac{dP2}{dt} &= [(1 - \gamma)\sigma_{P2} - m_P - v_{P2}/M]P2 - G_{Z1,P2}Z1 - G_{Z2,P2}Z2 \\ \frac{dZ1}{dt} &= (\beta G_{Z1,P1} + \beta G_{Z1,P2} + \beta G_{Z1,B} + \beta G_{Z1,D} - reg_{Z1} - m_{Z1}Z1)Z1 - G_{Z2,Z1}Z2 \\ \frac{dZ2}{dt} &= (\beta G_{Z2,P2} + \beta G_{Z2,Z1} + \beta G_{Z2,D} - reg_{Z2} - m_{Z2}Z2)Z2 \\ \frac{dB}{dt} &= (\sigma_{B,NH_4} + \sigma_{B,DON} - reg_B - m_B)B - G_{Z1,B}Z1 \\ \frac{dNO_3}{dt} &= -\sigma_{P1,NO_3}P1 - \sigma_{P2,NO_3}P2 - dil \times NO_3 \\ \frac{dNH_4}{dt} &= -\sigma_{P1,NH_4}P1 - \sigma_{P2,NH_4}P2 + (\epsilon reg_{Z1} + (1 - \Omega)m_{Z1}Z1)Z1 + (\epsilon reg_{Z2} + (1 - \Omega)m_{Z2}Z2)Z2 + (reg_B - \sigma_{B,NH_4})B \\ \frac{dDON}{dt} &= \gamma\sigma_{P1}P1 + \gamma\sigma_{P2}P2 + (1 - \epsilon)reg_{Z1}Z1 + (1 - \epsilon)reg_{Z2}Z2 + m_D D + \dots + m_B B - \sigma_{B,DON}B \\ \frac{dD}{dt} &= ((1 - \beta)G_{Z1,P1} + (1 - \beta)G_{Z1,P2} + (1 - \beta)G_{Z1,B} - \beta G_{Z1,D} + \Omega m_{Z1}Z1)Z1 + \dots + ((1 - \beta)G_{Z2,P2} + (1 - \beta)G_{Z2,Z1} - \beta G_{Z2,D} \\ &\quad + \Omega m_{Z2}Z2)Z2 + m_{P1}P1 + m_{P2}P2 + \dots - (m_D + v_D/M)D \end{aligned}$$

M = mixed layer depth (MLD). G refers to the grazing of microzooplankton ($Z1$) or mesozooplankton ($Z2$) on respective prey items.

a Michaelis-Menten type equation as in [Fasham et al. \(1990\)](#), relating growth to prey concentration, a half-saturation constant for grazing, and food preferences.

2.3. Equations

A series of coupled differential equations described model flows, the basic structure of which was provided by [Fasham et al. \(1990\)](#) with several modifications. Model flows were modified to include two sizes each of phytoplankton and zooplankton ([Table 2](#)). Diatom sinking was added as a loss term to large phytoplankton and a contributor to vertical export. As well, the zooplankton equations were modified to accommodate advances in parameterization, specifically applying a quadratic mortality term to increase model stability (e.g., [Steele and Henderson, 1992](#); [Edwards and Yool, 2000](#)). Bacterial growth rates on NH_4 (σ_{B,NH_4}) and labile DON ($\sigma_{B,DON}$) were defined as in [Fasham et al. \(1990\)](#), but a mortality term was added for bacteria (m_B) which contributed to DON ([Anderson and Williams, 1998](#)). The concentration of sedimenting particles from the plume was quantified as the sum of sinking detritus and sinking diatoms. The models were integrated with Matlab 7.1 using the ode45 function—a numerical variable time step differential equation solver using a fifth order Runge–Kutta method.

2.4. Biological model parameters

When available, biological model parameters were determined from measurements in the MRP ([Table 1](#)). The initial slope of the photosynthesis–irradiance (P – E) curve (α) for phytoplankton was estimated by converting measurements in units of $mg\ C\ (mg\ Chl\ a)^{-1}\ (Ein\ m^{-2})^{-1}$ to modeled values in units of $d^{-1}\ (W\ m^{-2})^{-1}$. For April 1988, [Lohrenz et al. \(1990\)](#) reported mean α values in the three salinity sub-regions <20 , 20 – 30 , and >30 of 7.9 , 11.6 , and $16.6\ mg\ C\ (mg\ Chl\ a)^{-1}\ (Ein\ m^{-2})^{-1}$. We calculated an average α across salinities of $0.15\ d^{-1}\ (W\ m^{-2})^{-1}$, assuming phytoplankton carbon biomass to chlorophyll weight ratios

(C:Chl) of 20 , 30 , and 50 in each salinity region ([Breed et al., 2004](#)), the Redfield ratio for C:N = 6.6 ([Redfield et al., 1963](#)), and a PAR conversion factor of $1\ W\ m^{-2} = 4.15\ \mu Ein\ m^{-2}\ s^{-1}$ ([Morel, 1991](#)). Several model parameters were obtained from an April 2004 cruise in the plume (H. Liu and M. Dagg, unpublished data), including maximum specific small and large phytoplankton growth rates (3.12 and $3.36\ d^{-1}$), and a maximum $Z1$ grazing rate on $P1$ ($2.17\ d^{-1}$). A maximum $Z1$ grazing rate on $P2$ of $1.26\ d^{-1}$ was measured by [Liu and Dagg \(2003\)](#) on a March 2002 plume cruise. Initial values at zero salinity for certain compartments were chosen from springtime datasets as follows. The initial NH_4 concentration was set to $0.25\ \mu M$ based on plume measurements ([Gardner et al., 1997](#)). An initial labile DON concentration of $0.47\ \mu M$ was determined from an average spring concentration of total DON in the Mississippi River of $22.86\ \mu M$ (USGS data), assuming 2% lability ([Benner and Opsahl, 2001](#)). Unless otherwise noted, USGS data presented in this paper are for the St. Francisville, LA site for 1988–2003. Detrital concentration at zero salinity was calculated as $0.3\ \mu M$, as determined from mean Mississippi River particulate nitrogen concentrations ($14.7\ \mu M$; [Duan and Bianchi, 2006](#)) and a rough estimate of 2% lability, as for DON. Certain biological parameters and initial values were determined based on the fit between model results and a dataset of measurements collected during springtime.

Parameter values were obtained from the literature when measurements were not available ([Table 1](#)). Half-saturation constants for phytoplankton NO_3 and NH_4 uptake were chosen from [Walsh et al.'s \(2001\)](#) modeling study of the West Florida Shelf. This choice assumed that our large and small phytoplankton groups were represented by large diatoms ($K_{NO_3} = 1.7$; $K_{NH_3} = 2.0$) and *Synechococcus* ($K_{NO_3} = 0.2$; $K_{NH_3} = 0.1$), respectively. Other parameter choices are summarized in [Table 1](#), and were chosen from [Huret et al.'s \(2005\)](#) ecological model for the Río de la Plata plume, [Kelly-Gerrey et al.'s \(2004\)](#) model for the Irish Channel, and [Anderson and William's \(1998\)](#) model for the English Channel. Although we attempted to choose parameters from models for continental shelf regions, certain

parameters in these models are still often obtained from Fasham et al. (1990) and we did the same (Table 1). Preferences for mesozooplankton feeding on diatoms, microzooplankton, and detritus (0.7, 0.2, and 0.1) were chosen from Chai et al. (2002). We adopted the same preferences for microzooplankton feeding on small phytoplankton, bacteria, and detritus.

2.5. Model development and application

The model was developed through an iterative process by comparison of model results with plume measurements compiled from numerous springtime cruises. We refer to this measured data as the “optimization dataset”, since it was used to help develop the model and, hence, was not independent from model results. The model was initially developed for an average riverine NO_3 loading of $112 \mu\text{M}$, the long-term mean (USGS data). This is a scenario for which several data sets of plume measurements exist and against which model results were verified. Springtime measurements of chlorophyll *a* and NO_3 along a salinity transect were obtained from an April 1988 cruise for which riverine NO_3 was $107 \mu\text{M}$ (Lohrenz et al., 1999). Chlorophyll *a* was converted to phytoplankton biomass by assuming the same Chl:C ratios as described above. Plume bacterial concentrations were available from three cruises: May 1992 (Amon and Benner, 1998), April 2000 (Liu et al., 2004), and April 2004 (current study; methods as in Porter and Feig, 1980) for which riverine NO_3 concentrations were 214, 76, and $150 \mu\text{M}$, respectively. Bacterial concentration was relatively insensitive to riverine NO_3 inputs, as indicated by maxima at mid-salinities in all three datasets which were not significantly different ($1.5 \pm 0.2 \mu\text{M-N}$). Hence, all three datasets were used in our comparison with the $112 \mu\text{M}$ riverine NO_3 model output. Bacterial cell numbers were converted to nitrogen biomass using conversion factors of $20 \text{ fg C cell}^{-1}$ and a C:N weight ratio of 5 (Lee and Fuhrman, 1987). Measurements of micro- and mesozooplankton biomass were obtained from cruises in May 1993 (Strom and Strom, 1996), March 2002 (Liu and Dagg, 2003), and April 2004 (Sutor and Dagg, 2008; H. Liu, unpublished data). The riverine NO_3 concentrations for these cruises were 114, 120, and $150 \mu\text{M}$, respectively. Zooplankton biomass was converted to nitrogen biomass assuming 40% of dry weight as carbon and a C:N molar ratio of 6.625. Lastly, measurements of NH_4 along a salinity transect were obtained from a May 1992 cruise (Gardner et al., 1997) for which riverine NO_3 concentration was particularly high ($214 \mu\text{M}$). However, we felt that the careful methodology by which these samples were measured was most important in our choice of the dataset. Ammonium concentrations for this cruise were measured on board ship soon after sampling so that regeneration would not cause a problem in assessing the amounts that are actually in the water.

A partial validation of our model was performed through comparison of modeled and measured primary production at various riverine NO_3 loads. For comparison to measurements, modeled values of primary production were converted to $\text{g C m}^{-2} \text{ d}^{-1}$ using the Redfield ratio. In previous work, a relationship was demonstrated between measurements of primary production and riverine NO_x loading (Lohrenz et al., 1997), based on mean values of primary productivity calculated for a region around the delta. Although these measurements were from several seasons (spring–fall), we used them for comparison to model results, because there are currently not enough primary productivity measurements from only the spring to develop such a relationship with NO_3 loading. For comparison to measurements, an average value of modeled primary production was calculated across intermediate to high salinities (> 15), the region in which most measurements were made.

Our analysis of variable NO_3 loading on ecosystem functioning involves certain assumptions. First, it assumes changing nitrate concentrations under conditions of constant riverine discharge and constant initial conditions for the other eight nitrogen compartments. Second, using a nitrogen-based model assumes that other nutrients are not limiting. Although nitrogen often controls primary production in shelf waters near the Mississippi River delta, various studies provide evidence for limitation by phosphorus and silicate as well (e.g., Lohrenz et al., 1999 and references therein). More complicated multi-nutrient models would be useful for the plume, but they require data to parameterize which are not available, more assumptions, and are more difficult to interpret. While other nutrients may also be limiting in spring, our focus was to explore a simple nitrogen-based model first, and to provide a framework for more complex future models.

Our goal was to study the relationships between riverine NO_3 loading, primary production and sedimentation and to determine the main factors limiting these relationships. We studied the effects of NO_3 loading over a large range of riverine NO_3 inputs ($0\text{--}300 \mu\text{M}$); the observed springtime range is $64\text{--}213 \mu\text{M}$ (USGS data). At all NO_3 inputs, we analyzed changes in biomass, primary production, and sedimentation through the plume from zero salinity to the high salinity end-member; examples of this analysis are presented. As well, based on these modeled values, we calculated average values of biomass and rates of primary production and sedimentation over intermediate to high salinities (> 15), because we are primarily interested in plume contributions to organic matter cycling, rather than riverine. Average biomasses and rates were calculated by gridding modeled values to an evenly spaced salinity scale, followed by averaging of these gridded values from salinity 15 to 36. We simulated the specific case of a 30% decrease in NO_3 input to better understand the effects of the policy-mandated decrease in nitrogen loading to the Mississippi River watershed. The primary physical and biological factors regulating the relationship between NO_3 loading and rates were analyzed, including light limitation, nutrient limitation, residence time, diatom sinking, and grazing. Our approach was to decrease the role of each potential limiting factor and to observe its effect on the resulting relationships between NO_3 loading and ecosystem functioning. Specifically, five scenarios were modeled as follows: (1) dilution of NO_3 concentration was removed, (2) light attenuation by SPM and CDOM was removed by setting K_{abiotic} to that of water alone (0.046 m^{-1}), (3) light attenuation by mixing was reduced by setting MLDs to 1 m throughout the plume (4) residence time was increased by 50%, (5) diatom sinking was set to zero, and (6) all grazing rates were set to zero.

A sensitivity analysis was performed to determine which model parameters most affected modeled primary production and sedimentation. For $112 \mu\text{M}$ riverine NO_3 input, the sensitivity of both rates (in $\text{g N m}^{-2} \text{ d}^{-1}$) to small perturbations ($\pm 10\%$) in biological and physical model parameters (61 total) was assessed. An indicator of parameter sensitivity was calculated as $s = (\Delta r/r)/(\Delta p/p)$, where r is the rate of primary production (or sedimentation) at $112 \mu\text{M}$ riverine NO_3 , Δr is the change in primary production (or sedimentation) associated with a parameter change Δp , and p is the original parameter value. Values of $|s| > 1$ were considered to be sensitive to changes in the parameter.

3. Results

3.1. Model performance

The model was developed for a $112 \mu\text{M}$ riverine NO_3 scenario through comparison with plume measurements (the optimization

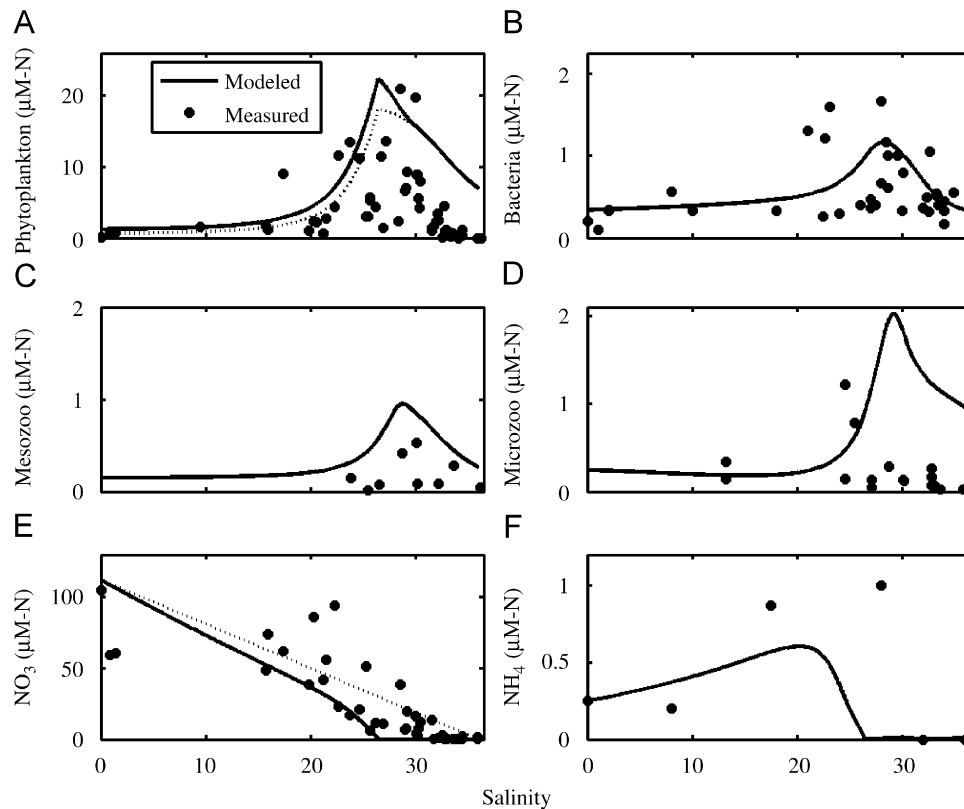


Fig. 3. Model verification for a 112 μM riverine NO_3 scenario through comparison with plume measurements of (A) phytoplankton, (B) bacteria, (C) mesozooplankton, (D) microzooplankton, (E) NO_3 , and (F) NH_4 concentrations. In the case of phytoplankton biomass, modeled values are a sum of the small (dashed line) and large phytoplankton groups. The conservative mixing relationship is shown for NO_3 (dashed line).

dataset; Fig. 3). Certain biological parameters, primarily for grazers, were determined based on which values gave an appropriate fit between model results and measurements (Table 1). For example, the highest measured mesozooplankton-grazing rate on the March 2002 cruise was 0.156 d^{-1} (Liu and Dagg, 2003). However, this value was not high enough to reproduce measured mesozooplankton biomasses and so we assumed a higher maximum mesozooplankton-grazing rate of 1.5 d^{-1} (Table 1). Similarly, we adopted a higher microzooplankton-mortality rate ($0.3 \text{ (d mmol m}^{-3}\text{)}^{-1}$) than in previous studies (e.g., $0.05 \text{ (d mmol m}^{-3}\text{)}^{-1}$; Merico et al., 2004), and a slightly higher mortality rate for mesozooplankton ($0.1 \text{ (d mmol m}^{-3}\text{)}^{-1}$), compared to $0.05 \text{ (d mmol m}^{-3}\text{)}^{-1}$ in Fasham et al. (1990). The initial concentrations of micro- and mesozooplankton at zero salinity were chosen to give appropriate model results at higher salinities, because no measurements of zooplankton biomass at low salinities are currently available. Initial concentrations of small and large phytoplankton ($0.60 \mu\text{M}$ each) and bacteria ($0.34 \mu\text{M}$) were chosen slightly above measured values so that peak biomass concentrations would be reached at intermediate, rather than high, salinities in the plume.

Excretion rates of NH_4 by bacteria, micro- and mesozooplankton were chosen based on the model's fit to plume measurements of NH_4 regeneration rates, NH_4 ambient concentrations, and biomasses. Mesozooplankton NH_4 excretion was set at 0.20 d^{-1} , which is twice that of the previously published value (0.1 d^{-1} ; Fasham et al., 1990). Significantly higher regeneration rates were adopted for bacteria and microzooplankton equal to 0.50 and 1.2 d^{-1} , respectively, based on reports of high regeneration in the plume region (Gardner et al., 1997). Isotope dilution experiments have shown that bacteria can contribute 7–50% of NH_4 regeneration in the plume in summer (Cotner and Gardner,

1993), such that grazers generally contribute more to regeneration except at intermediate salinities. Bacterial regeneration measurements in the spring plume showed that 20–50% of bacterial production can go to NH_4 regeneration (Jochem et al., 2004), so our 0.50 d^{-1} regeneration rate for bacteria is probably reasonable, given maximum bacterial growth rates of 2 d^{-1} in the model.

Model results for biomasses and nutrients generally fit measured values from the optimization dataset ($112 \mu\text{M}$ riverine NO_3 input; Fig. 3). In particular phytoplankton biomass was within range of measurements up to mid-salinities, but were at the upper end of measurements or above measured values at higher salinities (Fig. 3(A)). Modeled phytoplankton growth rates ranged from 0 to 1.52 d^{-1} and peaked at mid-salinities, comparing well with measured growth rates which ranged from -0.05 to 1.60 d^{-1} in March 2002 (Liu and Dagg, 2003) and from -0.13 to 3.15 d^{-1} in April 2004 (Liu and Dagg, unpublished). Modeled bacteria biomass was within range of measurements across all salinities (Fig. 3(B)). Modeled concentrations for mesozooplankton were slightly above measurements for the mid- to high salinities where they were available (Fig. 3(C)). Modeled microzooplankton biomass was within range of measurements through intermediate salinities, but was higher than measurements at high salinities (Fig. 3(D)). The precise location of the modeled microzooplankton peak relative to measurements is not particularly important, since the salinity at which biomass peaks can vary between cruises (even in the same season). At certain salinities, model results were at the extreme limits of measured data. Modeled phytoplankton biomass was towards the high end of measurements at higher salinities, causing NO_3 values to be at the low end of measured values due to phytoplankton uptake (Fig. 3(E)). Although NH_4 measurements were sparse, modeled concentrations of NH_4 were similar to measured values where

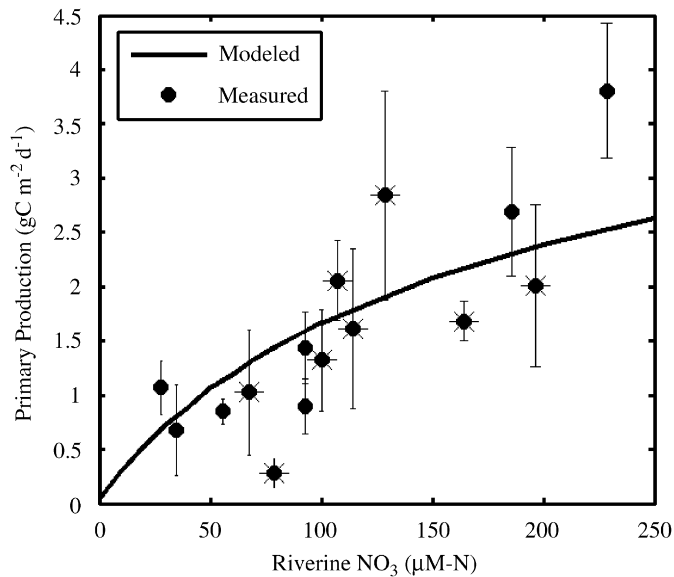


Fig. 4. Comparison of modeled and measured water-column-integrated primary production for variable riverine NO_3 loading. Modeled values are an average over intermediate to high salinities (>15), the region in which most measurements were made. Measurements are an average of data collected around the delta in multiple years and seasons (Lohrenz et al., 1997); spring (March–May) measurements are indicated by asterisks. Error bars on measured values indicate ± 1 SE.

data were available, including reproduction of a peak in concentration at intermediate salinities and a drop to undetectable levels at high salinities (Fig. 3(F)).

We compared modeled and measured primary production for a range of riverine NO_3 inputs. This comparison allowed for a partial validation of our model, showing good comparison between modeled water-column-integrated primary production and an independent dataset of measurements (Fig. 4; Lohrenz et al., 1997). Modeled values suggested a decreasing change in primary productivity with increasing NO_3 loads, well fit by a second order polynomial (Fig. 4; $\text{PP} = -3.80 \times 10^{-5} [\text{NO}_3]^2 + 1.92 \times 10^{-2} [\text{NO}_3] + 0.141$, where $[\text{NO}_3]$ is in $\mu\text{M-N}$ and PP is primary productivity in $\text{gC m}^{-2} \text{d}^{-1}$). This leveling off of modeled primary production at high NO_3 inputs was caused by the leveling off of phytoplankton growth rates. Measured data points consisted of a single average value calculated for each cruise from a set of locations which varied between cruises (Lohrenz et al., 1997). We included all available productivity measurements in our analysis which encompassed data from spring through fall. There are currently not enough spring measurements to know the exact relationship between primary production and NO_3 , across a large range of riverine NO_3 inputs for that particular season. Our modeled primary productivities also resulted in small phytoplankton contributing from 77% to 80% of average productivity (salinity >15) for NO_3 inputs of 10–250 μM . This contribution by small phytoplankton is at the high end of measurements of productivity which showed they contributed 40–70% in March 1991 (Redalje et al., 1994). Although aspects of the model could be improved, the relatively good fit between modeled and measured datasets gave us confidence in applying our ecosystem model to studying the impact of variable riverine NO_3 loading on primary productivity and sedimentation in the plume.

3.2. Effects of variable nitrate loading

The model was forced with variable riverine NO_3 concentrations to analyze the effects on ecosystem functioning. Decreased NO_3 loading resulted in substantial reductions in phytoplankton

biomass, primary production, and sedimentation at salinities >20 (Fig. 5), where nutrient limitation becomes more important than light limitation in determining phytoplankton growth. Variable NO_3 loading also affected the spatial location of biomass and primary production maxima, shifting them towards lower salinities with decreasing NO_3 concentrations; this shift was less pronounced for sedimentation (Fig. 5). For an order of magnitude decrease in NO_3 loading (from 250 to 25 μM), average biomasses for small phytoplankton (for salinity >15) decreased by ~ 4 times, and all other biomasses decreased by ≤ 2 times. Substantial decreases were also observed in rates with average primary production decreasing by 4 times and sedimentation by 3 times. Changes in phytoplankton size structure with variable NO_3 loading were observed for biomass, primary production, and sedimentation (Fig. 5(D)–(F)). Small increases in the contribution of large phytoplankton to average primary production and sedimentation were observed at higher NO_3 inputs. However, the observed impacts of NO_3 loading on size structure were dampened due to diatom sinking. Removal of diatom sinking from our model resulted in more pronounced contributions by large phytoplankton to biomass, primary production, and sedimentation at higher NO_3 loads.

Depending on salinity, different biological processes are the primary contributors to vertical export of labile PON from the plume mixed layer. For a riverine NO_3 input of 112 μM , total vertical export peaked at intermediate to high salinities due to high primary productivity and grazing in the plume, followed by a secondary peak at zero salinity from river borne PON (Fig. 6). Primary contributions to sedimentation were diatom sinking and microzooplankton egestion, followed by small phytoplankton mortality. At low salinities, both diatom sinking and microzooplankton egestion played a role in determining vertical export, with microzooplankton removing river borne particles from the mixed layer. At intermediate salinities, diatom sinking was the main contributor to sedimentation from the plume. Following a peak in primary production, microzooplankton egestion became the most important contributor to sedimentation at higher salinities and small phytoplankton mortality was the second most important contributor. Other biological processes played a more minor role in determining sedimentation, including mesozooplankton egestion, mortality of diatoms, micro- and mesozooplankton, and detrital breakdown to DON (Fig. 6).

Our primary goal was to model the relationship between riverine NO_3 loading, primary production and sedimentation, and to study the factors controlling this relationship. For the NO_3 loadings that we analyzed (0–300 μM), both primary production and sedimentation continued to increase throughout the entire range (Fig. 7(A)). However, primary production increased significantly more than did sedimentation, resulting in a ratio of sedimentation to primary production that ranged from 65% at a 1 μM NO_3 input to 17% at a 300 μM NO_3 input (Fig. 7(B)). For the range of measured springtime NO_3 loads (65–215 μM), changes in the ratio of sedimentation to primary production were small (19–23%). Recall that these percentages are an average over intermediate to high salinities (>15). Significant variability in the ratio was observed with salinity. For example for a 112 μM NO_3 load, the ratio ranged from 7% to 87% at intermediate salinities, and was fairly constant ($\sim 53\%$) at higher salinities where nitrogen limited phytoplankton growth (Fig. 7(C)). We also compared modeled ratios to May 1992 measurements (Redalje et al., 1994), for the same NO_3 input and salinity range as the measurements. The modeled ratio of sedimentation to primary production averaged 34%, which was somewhat less than the measured ratio in this region of 50%, but modeled values also varied widely in this salinity range (8–67%). For the range of measured springtime NO_3

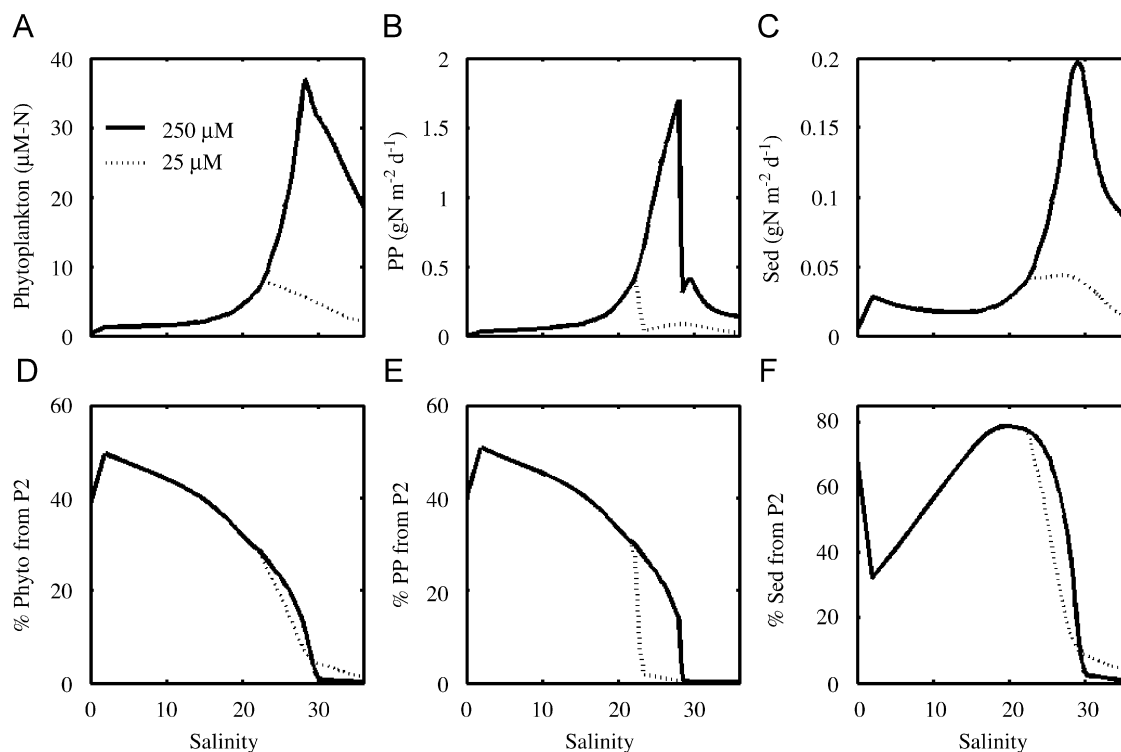


Fig. 5. Property-salinity relationships showing the effect of variable NO₃ loading on (A) phytoplankton biomass, (B) primary production (PP), and (C) sedimentation (Sed). As well, the percent contribution of large phytoplankton to (D) biomass and (E and F) rates is shown. Two NO₃ loading scenarios of 25 and 250 μM are compared.

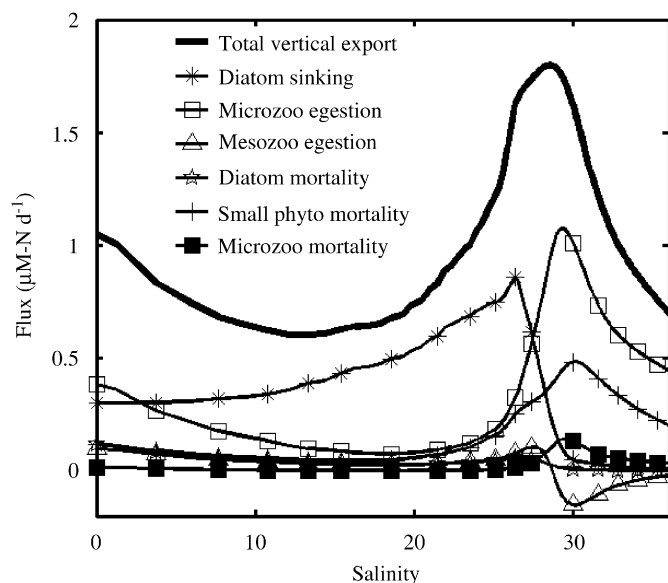


Fig. 6. Vertical export of PON from the mixed layer, and contributions of various processes to sedimentation, for 112 μM riverine NO₃ input. Diatom sinking contributes directly to vertical export, whereas the other processes (mortality and zooplankton feeding losses) all contribute to the detrital pool, a fraction of which is exported vertically. Contributions to vertical export by mesozooplankton mortality and detrital breakdown to DON were not included in the figure, because they were relatively minor compared to other processes. The contribution of mesozooplankton egestion to detrital vertical export can be negative, because mesozooplankton consume detritus and so remove particles from the sinking particulate pool.

loads, the following equations well described relationships between NO₃ load and average rates: $PP = -5.34 \times 10^{-6} [NO_3]^2 + 3.07 \times 10^{-3} [NO_3] + 3.30 \times 10^{-2}$ and $Sed = 6.93 \times 10^{-3} [NO_3]^{0.455}$, where PP and Sed are primary production and

sedimentation, respectively, in gN m⁻² d⁻¹ and [NO₃] is in μM-N. With relevance to nitrogen loading reductions to the Mississippi River watershed, a 30% decrease in NO₃ input to the plume (below 112 μM NO₃ loading) decreased average primary production by 19% and average sedimentation by 14% (Fig. 7(D)). A 40% decrease in NO₃ loading, as proposed by Scavia et al. (2003), decreased modeled primary production and sedimentation by 28% and 20%, respectively.

We analyzed the importance of several limiting factors on determining the relationships between NO₃ loading and ecosystem rates. The original model was compared to model runs in which the effects of various physical factors and grazing were altered, including the effects of NO₃ dilution, abiotic light attenuation, light attenuation by mixing, residence time, diatom sinking, and grazing (see Section 2 for details). Dilution of NO₃ via physical mixing of riverine and oceanic end members had the greatest impact on limiting average phytoplankton biomass, primary production, and sedimentation (Fig. 8(A)–(C)). Over the measured range of springtime NO₃ loads, removal of NO₃ dilution resulted in average increases in modeled biomass, production, and sedimentation of 2.8, 2.1, and 1.6 times, respectively. The next most important factors limiting primary production were abiotic light attenuation, light attenuation by mixing, and diatom sinking. Only the first two of these factors limited sedimentation. For a 112 μM riverine NO₃ input, removal of NO₃ dilution resulted in increased primary production and sedimentation at higher salinities (>25), whereas decreased light limitation mainly resulted in increased rates at lower salinities (<30) (Fig. 8(D)–(F)). Although removal of diatom sinking increased average primary production (Fig. 8(B)), it had little effect on average values of sedimentation (Fig. 8(C)). This was the result of no diatom sinking initially decreasing sedimentation at lower salinities, but later resulting in higher sedimentation supported by higher rates of nutrient regeneration at a salinity of ~30 (Fig. 8(F)).

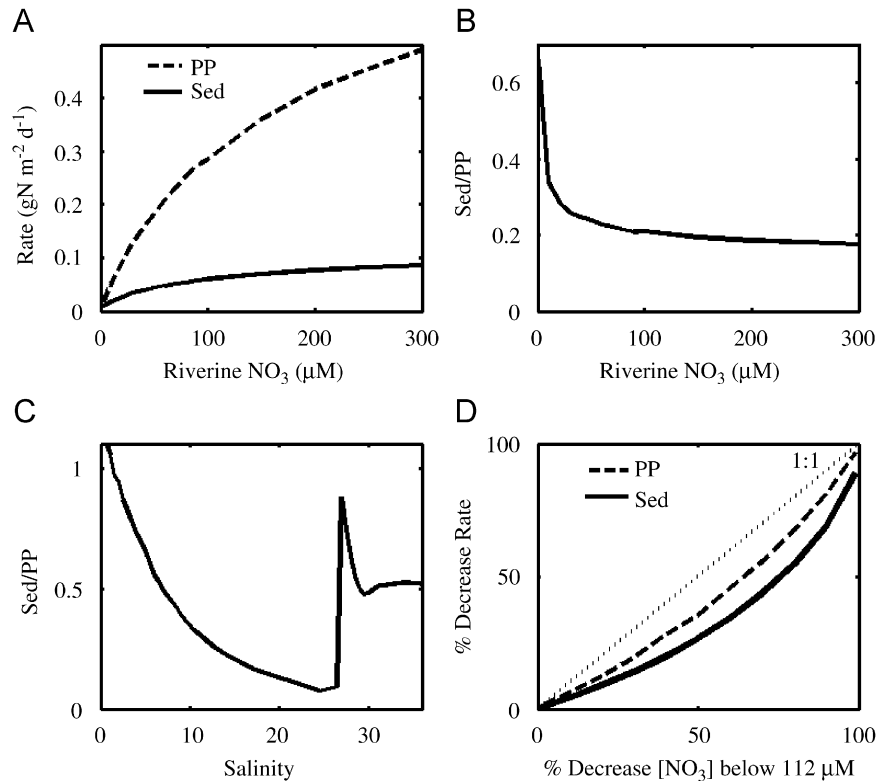


Fig. 7. Effect of variable riverine NO₃ loading on average rates of (A) primary production (PP) and sedimentation (Sed), and the ratio Sed/PP versus (B) NO₃ loads and (C) salinity. The example in panel C is for a NO₃ load of 112 μM (the long-term mean). As well, the relationship between decreasing NO₃ load and decreases in average primary production and sedimentation are shown (panel D). These decreases were calculated relative to a 112 μM NO₃ load scenario for which average primary production and sedimentation equaled 0.31 and 0.063 gN m⁻² d⁻¹, respectively. This panel addresses the potential impacts of mandated reductions in NO₃ loading to the Mississippi River watershed. For example, a 30% decrease in NO₃ below 112 μM would decrease average PP by 19% and average Sed by 14%. All average values of primary production and sedimentation were calculated for intermediate to high salinities (>15).

Grazing and residence time had more minimal impacts on ecosystem rates, and did not appear to be important limiting factors. The removal of grazing actually resulted in a slight decrease in average primary production across salinities (Fig. 8(B)). Although phytoplankton biomass increased at all salinities with grazing removed (Fig. 8(A)), phytoplankton growth rates and primary production decreased at higher salinities compared to the original model (Fig. 8(E)). The decrease in average primary production with grazing removed was due to nutrient limitation of phytoplankton growth at higher salinities in the absence of NH₄ regeneration by microzooplankton. The increase in phytoplankton biomass at all salinities with grazing removed (Fig. 8(A)) generally resulted in a slight increase in average sedimentation (Fig. 8(C)). Increased residence times lead to a decrease in biomass, productivity, and sedimentation (Fig. 8(A)–(C)), primarily caused by an increased amount of time spent at low to mid-salinities where light limitation of growth decreased phytoplankton growth rates and biomass, in comparison to the original model.

3.3. Sensitivity analysis

A sensitivity analysis was performed to determine the effect of small changes in each model variable on modeled outputs. For a 112 μM NO₃ load, the sensitivity factor, s , was calculated to describe the effect on modeled rates of a $\pm 10\%$ change in a parameter (see Section 2). Rates were considered sensitive to a parameter for values of $|s| > 1$ anywhere along the salinity gradient. A negative s value indicates that the change in rate has

the opposite sign as the parameter change. For example, a sensitivity of $s = 2$ shows that a 10% increase in the parameter results in a 20% increase in the rate, and a sensitivity of $s = -0.5$ shows that a 10% increase in the parameter results in a 5% decrease in the rate.

Primary production was generally more sensitive to perturbations in model parameters than was sedimentation. Of the 61 physical and biological parameters in the model, primary production was sensitive to 7 and sedimentation was sensitive to 4, with higher values of $|s|$ observed for primary production (Fig. 9). Highest sensitivities for both primary production and sedimentation were observed at intermediate to high salinities. Both modeled rates were sensitive to abiotic light attenuation ($K_{abiotic}$), microzooplankton excretion rate (reg_{Z1}), maximum growth rate of large phytoplankton ($\mu_{P2,max}$), and maximum grazing rate of microzooplankton on P1, B, and D ($g_{Z1a,max}$). In addition, primary production was sensitive to MLD, maximum growth rate of small phytoplankton ($\mu_{P1,max}$), and the assimilation efficiency of microzooplankton grazing on small phytoplankton ($\beta_{Z1 \text{ on } P1}$). The sensitivity of primary production to parameter changes varied with salinity, such that changes in $K_{abiotic}$ resulted in the highest sensitivity at low salinity, whereas perturbations in $\beta_{Z1 \text{ on } P1}$ were most important at high salinity (maximum $|s| = 3.8$). The most sensitive parameter for sedimentation was $\mu_{P2,max}$ (maximum $|s| = 2.6$); sensitivity to this parameter peaked at the same salinity as peak contributions of diatom sinking to sedimentation (Fig. 6). The second most sensitive parameter for sedimentation was $g_{Z1a,max}$, and its peak sensitivity likewise coincided with the peak contribution of microzooplankton egestion to sedimentation (Fig. 6). The highest sensitivities for

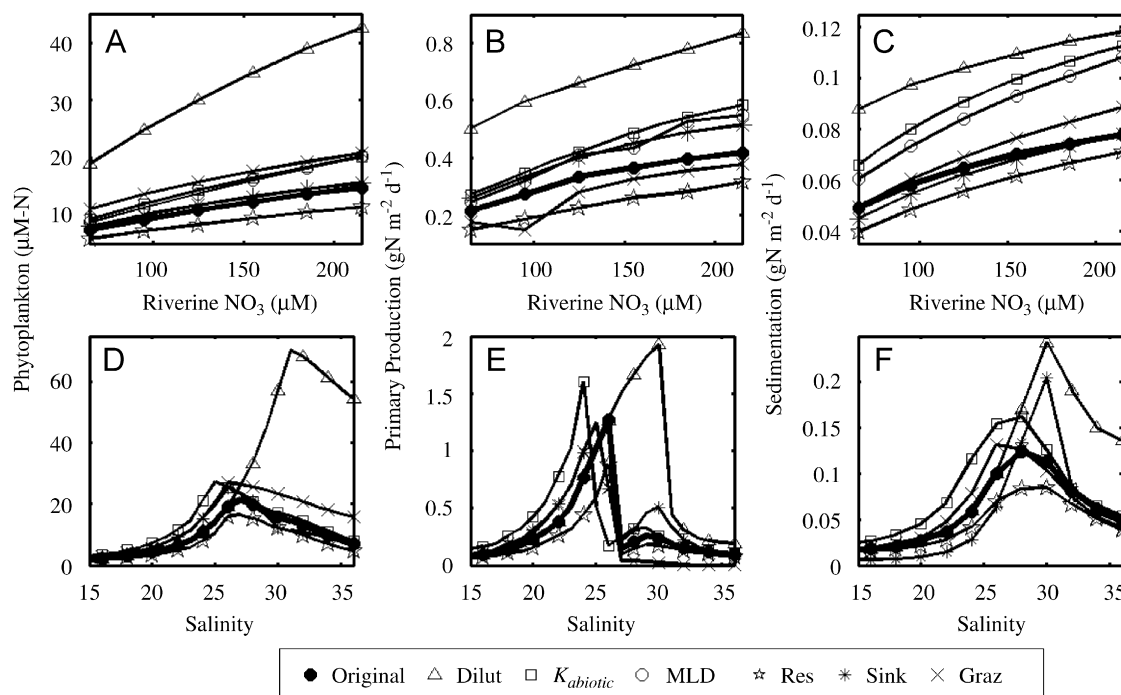


Fig. 8. Effects of various physical factors and grazing on the relationship between NO_3 loading, and average (A) phytoplankton biomass, (B) primary production, and (C) sedimentation. As well, for a $112 \mu\text{M}$ NO_3 load, the relationships between salinity and (D) phytoplankton biomass, (E) primary production, and (F) sedimentation are shown. We compared the original model to simulations in which the effects of various factors were modified as follows: (1) dilution of NO_3 was removed (“Dilut”), (2) abiotic light attenuation by SPM and CDOM was removed by setting $K_{abiotic}$ to that of water alone (0.046 m^{-1} ; “ $K_{abiotic}$ ”), (3) light attenuation by mixing was reduced by setting mixed layer depths to 1 m (“MLD”), (4) residence time was increased by 50% (“Res”), (5) diatom sinking was set to zero (“Sink”), and (6) all grazing rates were set to zero (“Graz”). For clarity, a subset of symbols is plotted in all panels, and low salinities are not shown in panels D–F. As well, the “MLD” scenario has not been plotted in panels D–F, because the trends are similar to the “ $K_{abiotic}$ ” scenario.

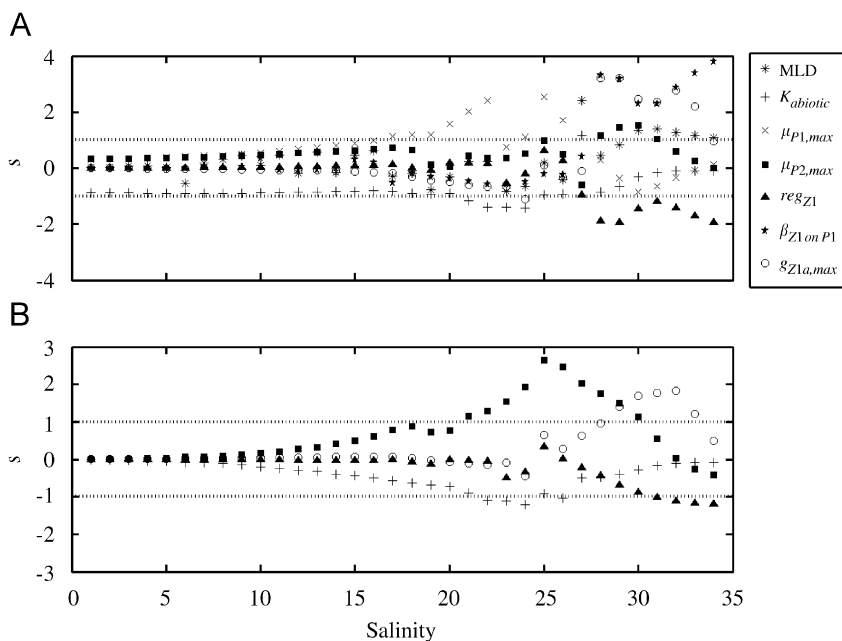


Fig. 9. Sensitivity to 10% increases in model parameters of (A) primary production and (B) sedimentation, for a $112 \mu\text{M}$ riverine NO_3 scenario. All parameters for which primary production and sedimentation were sensitive ($|s| > 1$; dotted lines) are plotted. For brevity, the sensitivities to -10% changes in model parameters are not shown.

both primary production and sedimentation were to biological parameters (e.g., microzooplankton grazing and phytoplankton growth) rather than to physical parameters (e.g., MLD, $K_{abiotic}$, or residence time).

For the majority of model parameters, low sensitivity ($|s| < 1$) of modeled rates was observed. For example, low sensitivity was

observed for all initial concentrations, mesozooplankton and bacterial growth parameters, and half-saturation constants for phytoplankton nutrient uptake. Though neither diatom or detrital sinking speeds were sensitive parameters, we wanted to analyze their impacts on sedimentation further because of the range of values reported in the literature. When we adopted an alternative

diatom sinking speed of 0.5 m d^{-1} (e.g., Anderson and Williams, 1998) versus the 1 m d^{-1} in our model, then average sedimentation at intermediate to high salinities (>15) increased by 8% compared to the original model. We also adopted two alternative detrital sinking speeds of 1 m d^{-1} (e.g., Merico et al., 2004) and 10 m d^{-1} (e.g., Anderson and Williams, 1998). For these two scenarios, average sedimentation decreased by 48% and increased by 4%, respectively, such that significantly more sensitivity was observed in decreases to the detrital sinking speed than to increases. Hence, large decreases in detrital sinking speed from what we have assumed in the model, but within a plausible range of literature values, can have significant effects on sedimentation. Ideally, different detrital sinking speeds would be adopted depending on particle size and composition, however, significantly more data will be needed to constrain such parameterizations in ecosystem models.

4. Discussion

4.1. Implications for nitrate loading reduction

Ecosystem model results for the MRP indicated that for a given percent decrease in riverine NO_3 loading, about half of that decrease could be expected in average plume sedimentation of organic matter. For example, a 30% reduction in NO_3 loading lead to decreases in average primary production (for salinity >15) of 19% and sedimentation of 14%, and for a 40% reduction in NO_3 loading, primary production and sedimentation decreased by 28% and 20%, respectively (Fig. 7(D)). The importance of this finding is to illustrate the dampening effects that physical processes (e.g., light attenuation and dilution) and food web interactions have on the conversion of river borne nutrients to sedimenting organic matter in Louisiana shelf waters. Similarly, other modeling studies have shown the effects of limiting factors on the relationship between nutrient loading and organic matter production in coastal ecosystems. For example, a biophysical model for the North Sea demonstrated that a 50% reduction in nitrogen and phosphorus loads could result in decreases of 5–30% in primary production depending on location (Skogen et al., 2004). A study of nutrient abatement in the Baltic Sea, using a 3-D ecosystem model, showed that a reduction of riverine nitrogen and phosphorus loading by 50% ultimately lead to a 10% decrease in chlorophyll concentration in the Central Baltic (Neumann and Schernewski, 2005). As observed for the North Sea, natural variability due to forcing fields other than nutrients (e.g., changing weather) can often exceed the modeled changes in primary productivity that are expected following nutrient reduction (Skogen et al., 2004). This is likely the case in the MRP for the proposed 30% reductions in NO_3 loading to the watershed. Modeled changes in plume primary production (–19%) are relatively small compared to natural variability in plume primary productivity measurements, as seen in April 1988 when measurements often showed a two-fold variation at any given salinity (Lohrenz et al., 1990). MLD and abiotic light attenuation are examples of two forcing fields in the plume that show variability (Fig. 2(B) and (C)) and for which rates were sensitive (Fig. 8) that could potentially mask the effects of 30% reductions in NO_3 loading.

The fraction of organic matter production that sediments from plume surface waters is an important quantity in relating nutrient loading to hypoxic zone size, however this ratio is highly variable in river-dominated waters. For a $112 \mu\text{M}$ NO_3 input, our model showed that the ratio of sedimentation to primary production ranged widely (7–87%) at intermediate to high salinities in springtime. Such a large range in ratios for the plume has

previously been reported in both modeling studies (Green et al., 2006) and measured data (Redalje et al., 1994), though at coarser scales of salinity resolution. Our current model shows that this large range of ratios was primarily caused by the lag between high rates of primary production in the plume and high rates of sedimentation (Figs. 5 and 7). Predictive models of the relationship between riverine NO_3 loading and Louisiana–Texas shelf hypoxic zone size, often assume that a constant 50% of primary production is exported below the pycnocline regardless of season or salinity (e.g., Rabalais et al., 1991; Scavia et al., 2003). Our results indicate that sensitivity analyses should be performed with these predictive models of hypoxia size to better understand the effect of variability in this ratio. Results from our current model suggest that the mean ratio of export to primary production is $\sim 14\%$ at intermediate salinities where nitrogen is available to support primary production and diatom sinking is the major contributor to sedimentation (Figs. 6 and 7). However, this modeled ratio is higher and averages $\sim 53\%$ at higher salinities (>27) where phytoplankton growth is nitrogen limited and contributions from microzooplankton egestion and small phytoplankton mortality are most important to sedimentation (Fig. 6). Hence, at higher salinities predictive models of hypoxia size may be right in assuming a ratio of 50%, but care needs to be taken regarding which salinities are most pertinent in these models. For example, if a broader range of salinities (>15) is most important to such modeling efforts, then our results suggest that a lower ratio of $\sim 20\%$ is more representative of organic matter export from the plume's food web.

4.2. Factors limiting phytoplankton growth and sedimentation

One of our objectives was to better understand the primary controls on relationships between NO_3 loading and plume ecosystem functioning. While it is generally known that phytoplankton growth is limited by light availability at low salinities and nutrient availability at high salinities in the plume, the role of these processes in concert with biological factors, such as grazing, has not been quantitatively studied. Based on our model results, physical attributes of the plume were most important in shaping the response of changes in primary production and sedimentation to variable NO_3 loading. The primary limiting factor of average biomass, primary production, and sedimentation was the physical dilution of NO_3 (Fig. 8(A)–(C)). The effects of dilution on ecosystem response to nutrient loading were also documented in a modeling study of waters in the archipelago off Helsinki, where nutrient transport and dilution into a large area contributed to negligible impacts on algal biomass of proposed reductions in nutrient loads (Korpinen et al., 2004). In our plume model, secondary controlling factors of average primary production were abiotic light attenuation, light attenuation due to mixing, and diatom sinking, with only the first two of these factors playing a role in limiting sedimentation. The importance of physical factors such as nutrient and light limitation in controlling phytoplankton growth in the plume has previously been documented. Lohrenz et al. (1990) presented several lines of evidence for nitrogen limitation of primary production at high salinities, including: (1) the depletion of nitrogen at salinities less than the Gulf water end-member, (2) maxima in phytoplankton production and biomass occurring at salinities just below the range of nitrogen depletion, and (3) approximate calculations of mixed layer integrated production which suggested that biological consumption was comparable to riverine nitrogen inputs. In a comparison of observed chlorophyll concentrations and those predicted using a steady-state light limitation model, the authors also showed that light availability constrained levels of primary

production in some regions of the plume. In an analysis of springtime (March–May) Mississippi River suspended sediment loads (USGS data, 1980–2005), we found evidence that suspended sediment concentrations have decreased since 1980, which according to our model should have increased plume primary production and been a contributing factor to increased hypoxia size during that time.

In addition to nutrient and light limitation, we explored the importance of other factors in controlling primary production and sedimentation in the plume. Lohrenz et al. (1990) found that both light and nutrients were adequate to support growth beyond observed levels at intermediate and low salinities, such that other factors were required to explain observed patterns of biomass and production along the MRP/oceanic gradient. The authors suggested that these other factors might include limitation by trace elements (such as Fe) needed for phytoplankton growth, higher phytoplankton mortality due to grazing, respiration, or sinking, and the inhibition of growth due to metal toxicity or steep salinity gradients. The only additional limiting factor of plume primary production that we were able to identify with our model was that of diatom sinking. With diatom sinking removed, average primary production increased by 20–24% in the plume for the observed range of riverine NO₃ loads (Fig. 8(B)), whereas the effects on sedimentation were more minor, with increases of 0–9% (Fig. 8(C)). Zooplankton grazing, as parameterized in our current model, did not have a limiting effect on primary production or sedimentation, but rather acted to increase both rates. The primary reason for decreased primary production with grazing removed from the model was due to the removal of NH₄ excretion by microzooplankton which otherwise supports small phytoplankton growth at higher salinities (Fig. 8(E)). Regarding plume residence times, Lohrenz et al. (1990) previously suggested that short plume residence times might act to limit phytoplankton growth, however we did not find evidence that residence time, as parameterized in our model, limited primary productivity or sedimentation in the plume. There are few measurements of plume transit times, and the current model would certainly change if substantially different transit times were found to be more accurate for the spring season. However, in our model neither primary production nor sedimentation was sensitive to small changes in residence time (Fig. 9).

4.3. Model applicability and limitations

The springtime ecosystem model presented here for the MRP has certain limitations. The model employs relatively basic physics, including average daily light levels (versus a day-night light cycle), no mixing between the surface plume and lower water column, and approximate residence times. In addition, the dynamics of frontal processes were not incorporated into the current model, even though there is evidence that hydrodynamic processes at ephemeral turbidity fronts play a role in structuring plume population densities (Govoni and Grimes, 1992). It is impossible to set up a perfectly realistic biological model, and we made several simplifications, such as the assumption of homogeneity throughout the mixed layer. Subsurface biomass maxima have been observed in regions of strong vertical density gradients in the plume (Lohrenz et al., 1999), however, their impact on nutrient cycling and food web dynamics were averaged into the current model. Incorporating such features would require more data and a vertically resolved physical model. We assumed continuity in biological species composition across the salinity regime (0–36). In reality, at low salinities there would be a change in community composition from freshwater to saltwater tolerant species. Most likely, those species that lack saltwater tolerance

sink out of the plume at low salinities and are replaced by living marine species that mix upward from bottom waters. However, since there is no evidence of an abrupt loss of freshwater cells followed by slow replacement of marine cells, our assumption of continuity must suffice in the current model.

Aggregation processes resulting in floc formation can be an important contributor to vertical export from surface waters. Flocculation occurs when particles in suspension clump together into rapidly sinking aggregates of many particles called “flocs”. Aggregation was not incorporated into our current ecosystem model though there are indications that this process may be particularly important during phytoplankton blooms. As well, phytoplankton biomasses obtained from our model were at the high end of measurements for intermediate to high salinities (Fig. 3(A)), suggesting there is a process at work, such as aggregation, which has not been included in the current model. Jackson (1990) modeled the dynamics of an algal bloom using coagulation theory and algal growth kinetics, and the results described a two-state system in which coagulation processes were unimportant at low algal concentration, but dominated at high algal concentrations. A coagulation dynamics model was also combined with the food web model of Fasham et al. (1990), and showed that coagulation can have an important effect on particle flux even in the low particle concentration oligotrophic environment (Jackson, 2001). Integration of the coagulation and NPZ models relied upon incorporation of many new variables into the ecosystem model, including, for example, those related to particle size spectra and mass, collision rates based on Brownian motion, shear, and differential sedimentation, and the subdivision of dissolved organic matter release into a colloidal fraction and a truly dissolved fraction. Based on model results, one of the author’s conclusions was that it is premature to use simple parameterizations, such as those relating particle concentration and removal rate, to represent the effect of coagulation in planktonic food webs. For these reasons, we have not incorporated aggregation processes into our current ecosystem model, though they are likely to be important.

Despite known simplifications, the ecosystem model generally represented measured population dynamics in the MRP. The model was forced by the best estimates of residence time, light attenuation, and MLDs currently available (Fig. 1). Modeled biomasses of bacteria, phytoplankton, and micro- and mesozooplankton across the salinity gradient well matched the measured values from which model parameters were developed (Fig. 3). Additionally, modeled changes in primary production with variable NO₃ loading were within range of measured values from an independent dataset (Fig. 4). Perhaps the least data were available for grazers, and future model development would benefit from measurement of zooplankton densities at lower salinities (<20; Fig. 3(C) and (D)), as well as a better understanding of grazing as a function of food concentration in high turbidity environments (e.g., ingestion half-saturation constants and maximum grazing rates). However, the availability of both micro- and mesozooplankton biomasses and grazing rates for the MRP is unique in comparison to the three other river plumes discussed in this issue, those of the Pearl, Yangtze, and Rhone. Although microzooplankton measurements are lacking in the other river plumes, measurements of mesozooplankton do exist and have shown, for example, large variations between the flood and dry seasons in the Pearl River estuary (Tan et al., 2004) and the Yangtze River plume (see Dagg et al., 2004 for references), and the importance of mesozooplankton migration in the Rhone River plume (Pagano et al., 1993). We suggest that measurement of microzooplankton grazing would be a key factor in the development of similar ecosystem models for the Pearl, Yangtze, and Rhone River plumes.

5. Conclusions

We developed a springtime, nitrogen-based ecosystem model for the immediate Mississippi River plume. The model incorporated nine biological compartments and physical forcing by photosynthetically active radiation, in-water light attenuation, residence time, mixed layer depths, and dilution. The model reproduced a dataset of biological measurements from which the model was developed, as well as an independent dataset of primary productivity measured at variable riverine NO_3 loadings. Three major conclusions were drawn from application of this model to better understanding the relationship between riverine NO_3 loading and organic carbon production and sedimentation in the plume. First, the percent decrease in primary production and sedimentation from the plume was significantly less than the percent decrease in riverine NO_3 input, such that a 30% decrease in NO_3 resulted in a 19% decrease in primary production and a 14% decrease in sedimentation. Second, the limiting factors of the relationship between NO_3 and primary production were NO_3 dilution primarily, followed by abiotic light attenuation, light attenuation due to mixing, and diatom sinking. Sedimentation was primarily limited by the first three of these factors. Third, our model results indicate that the fraction of primary production exported from the mixed layer is highly variable with salinity, and that predictive models of hypoxic zone size should consider this when assuming a constant value for this ratio. Interesting future directions with ecosystem models for the Mississippi River plume would be to incorporate limitation by nutrients other than nitrogen (e.g., phosphorus and silicate), include aggregation processes, and integrate a fully 3-D physical model, as mixing and dilution are clearly major factors regulating ecosystem functioning.

Acknowledgments

We sincerely thank Hongbin Liu and Malinda Sutor for making available plume mesozooplankton and microzooplankton data. We also thank Tom Bianchi who provided helpful comments and support. Fei Chai and Brad Penta provided helpful advice on ecosystem model development. The manuscript was significantly improved during the review process by Masahiko Fujii and two anonymous reviewers. This work was funded by the EPA and Louisiana Board of Regents Agreement Number R-82942001.

References

- Amon, R.M.W., Benner, R., 1998. Seasonal patterns of bacterial abundance and production in the Mississippi River plume and their importance for the fate of enhanced primary production. *Microbial Ecology* 35, 289–300.
- Anderson, T.R., Williams, P.J.B., 1998. Modelling the seasonal cycle of dissolved organic carbon at station E1 in the English Channel. *Estuarine, Coastal, and Shelf Science* 46, 93–109.
- Benner, R., Opsahl, S., 2001. Molecular indicators of the sources and transformations of dissolved organic matter in the Mississippi River plume. *Organic Geochemistry* 32, 597–611.
- Bierman Jr., V.J., Hinz, S.C., Zhu, D.-W., Wiseman Jr., W.J., Rabalais, N.N., Turner, R.E., 1994. A preliminary mass balance model of primary productivity and dissolved oxygen in the Mississippi River plume/Inner Gulf Shelf region. *Estuaries* 17, 886–899.
- Breed, G.A., Jackson, G.A., Richardson, T.L., 2004. Sedimentation, carbon export and food web structure in the Mississippi River plume described by inverse analysis. *Marine Ecology Progress Series* 278, 35–51.
- Chai, R., Dugdale, R.C., Peng, T.-H., Wilkerson, F.P., Barber, R.T., 2002. One-dimensional ecosystem model of the equatorial Pacific upwelling system. Part I: model development and silicon and nitrogen cycle. *Deep-Sea Research II* 49, 2713–2745.
- Cotner Jr., J.B., Gardner, W.S., 1993. Heterotrophic bacterial mediation of ammonium and dissolved free amino acid fluxes in the Mississippi River plume. *Marine Ecology Progress Series* 93, 75–87.
- Dagg, M.J., 1995. Copepod grazing and the fate of phytoplankton in the northern Gulf of Mexico. *Continental Shelf Research* 15, 1303–1317.
- Dagg, M., Benner, R., Lohrenz, S., Lawrence, D., 2004. Transformation of dissolved and particulate materials on continental shelves influenced by large rivers: plume processes. *Continental Shelf Research* 24, 833–858.
- Duan, S., Bianchi, T.S., 2006. Seasonal changes in the abundance and composition of plant pigments in particulate organic carbon in the lower Mississippi and Pearl Rivers. *Estuaries and Coasts* 29, 427–442.
- Edwards, A.M., Yool, A., 2000. The role of higher predation in plankton population models. *Journal of Plankton Research* 22, 1085–1112.
- Fasham, M.J.R., Ducklow, H.W., McKelvie, S.M., 1990. A nitrogen-based model of plankton dynamics in the oceanic mixed layer. *Journal of Marine Research* 48, 591–639.
- Gardner, W.S., Cavaletto, J.F., Cotner, J.B., Johnson, J.R., 1997. Effects of natural light on nitrogen cycling rates in the Mississippi River plume. *Limnology and Oceanography* 42, 273–281.
- Gordon, H.R., Brown, O.B., Evans, R.H., Brown, J.W., Smith, R.C., Baker, K.S., Clark, D.K., 1988. A semi-analytic radiance model of ocean color. *Journal of Geophysical Research* 93, 10909–10924.
- Govoni, J.J., Grimes, C.B., 1992. The surface accumulation of larval fishes by hydrodynamic convergence within the Mississippi River Plume front. *Continental Shelf Research* 12, 1265–1276.
- Green, R.E., Bianchi, T.S., Dagg, M.J., Walker, N.D., Breed, G.A., 2006. Application of an organic carbon budget for the Mississippi River turbidity plume to air-sea CO_2 fluxes and bottom-water hypoxia. *Estuaries and Coasts* 29, 579–597.
- Huret, M., Dadou, I., Dumas, F., Lazure, P., Garçon, V., 2005. Coupling physical and biogeochemical processes in the Río de la Plata plume. *Continental Shelf Research* 25, 629–653.
- Jackson, G.A., 1990. A model of the formation of marine algal flocs by physical coagulation processes. *Deep-Sea Research* 37, 1197–1211.
- Jackson, G.A., 2001. Effect of coagulation on a model planktonic food web. *Deep-Sea Research* 48, 95–123.
- Jerlov, N.G., 1976. *Marine Optics*. Elsevier, Amsterdam.
- Jochem, F.J., McCarthy, M.J., Gardner, W.S., 2004. Microbial ammonium cycling in the Mississippi River plume during the drought spring of 2000. *Journal of Plankton Research* 26, 1265–1275.
- Justić, D., Rabalais, N.N., Turner, R.E., 1997. Impacts of climate change on net productivity of coastal waters: implication for carbon budgets and hypoxia. *Climate Research* 8, 225–237.
- Justić, D., Rabalais, N.N., Turner, R.E., 2002. Modeling the impacts of decadal changes in riverine nutrient fluxes on coastal eutrophication near the Mississippi River Delta. *Ecological Modeling* 152, 33–46.
- Kelly-Gerrey, B.A., Anderson, T.R., Holt, J.T., Gowen, R.J., Proctor, R., 2004. Phytoplankton community structure at contrasting sites in the Irish Sea: a modelling investigation. *Estuarine, Coastal, and Shelf Science* 59, 363–383.
- Korpinen, P., Kiirikki, M., Koponen, J., Peltoniemi, H., Sarkkula, J., 2004. Evaluation and control of eutrophication in Helsinki sea area with the help of a nested 3D-ecohydrodynamic model. *Journal of Marine Systems* 45, 255–265.
- Lee, S., Fuhrman, J.A., 1987. Relationships between biovolume and biomass of naturally derived marine bacterioplankton. *Applied Environmental Microbiology* 53, 1298–1303.
- Leming, T.D., Stuntz, W.E., 1984. Zones of coastal hypoxia revealed by satellite scanning have implications for strategic fishing. *Nature* 310, 136–138.
- Liu, H., Dagg, M., 2003. Interactions between nutrients, phytoplankton growth, and micro- and mesozooplankton grazing in the plume of the Mississippi River. *Marine Ecology Progress Series* 258, 31–42.
- Liu, H., Dagg, M., Campbell, L., Urban-Rich, J., 2004. Picophytoplankton and bacterioplankton in the Mississippi River plume and its adjacent waters. *Estuaries* 27, 147–156.
- Lohrenz, S.E., Dagg, M.J., Whitledge, T.E., 1990. Enhanced primary production at the plume/oceanic interface of the Mississippi River. *Continental Shelf Research* 10, 639–664.
- Lohrenz, S.E., Fahnenstiel, G.L., Redalje, D.G., Lang, G.A., Chen, X., Dagg, M.J., 1997. Variations in primary production of northern Gulf of Mexico continental shelf waters linked to nutrient inputs from the Mississippi River. *Marine Ecology Progress Series* 155, 45–54.
- Lohrenz, S.E., Fahnenstiel, G.L., Redalje, D.G., Lang, G.A., Dagg, M.J., Whitledge, T.E., Dortch, Q., 1999. Nutrients, irradiance, and mixing as factors regulating primary production in coastal waters impacted by the Mississippi River plume. *Continental Shelf Research* 19, 1113–1141.
- Merico, A., Tyrrell, T., Lessard, E.J., Oguz, T., Stabeno, P.J., Zeeman, S.J., Whitledge, T.E., 2004. Modelling phytoplankton succession on the Bering Sea shelf: role of climate influences and trophic interactions in generating *Emiliania huxleyi* blooms 1997–2000. *Deep-Sea Research I* 51, 1803–1826.
- Morel, A., 1991. Light and marine photosynthesis: a spectral model with geochemical and climatological implications. *Progress in Oceanography* 26, 263–306.
- Neumann, T., Schernewski, G., 2005. An ecological model evaluation of two nutrient abatement strategies for the Baltic Sea. *Journal of Marine Systems* 56, 195–206.
- Pagano, M., Gaudy, R., Thibault, D., Lochet, F., 1993. Vertical migrations and feeding rhythms of mesozooplanktonic organisms in the Rhone River plume area (North-west Mediterranean Sea). *Estuary, Coastal and Shelf Science* 37, 251–269.
- Pakulski, J.D., Benner, R., Whitledge, T., Amon, R., Eadie, B., Cifuentes, L., Ammerman, J., Stockwell, D., 2000. Microbial metabolism and nutrient cycling

- in the Mississippi and Atchafalaya River plume. *Estuarine, Coastal and Shelf Science* 50, 173–184.
- Porter, K.G., Feig, Y.S., 1980. The use of DAPI for identifying and counting aquatic microflora. *Limnology and Oceanography* 25, 943–948.
- Rabalais, N.N., Turner, R.E., Wiseman Jr., W.J., Boesch, D.F., 1991. A brief summary of hypoxia on the northern Gulf of Mexico continental shelf: 1985–1988. In: Tyson, R.V., Pearson, T.H. (Eds.), *Modern and Ancient Continental Shelf Anoxia*. Geological Society Special Publication No. 58, London, pp. 35–47.
- Rabalais, N.N., Turner, R.E., Wiseman Jr., W.J., 2002. Gulf of Mexico hypoxia, a.k.a. “The Dead Zone”. *Annual Review of Ecology and Systematics* 33, 235–263.
- Redalje, D.G., Lohrenz, S.E., Fahnenstiel, G.L., 1994. The relationship between primary production and the vertical export of particulate organic matter in a river-impacted coastal ecosystem. *Estuaries* 17, 829–836.
- Redfield, A.C., Ketchum, B.H., Richards, F.A., 1963. The influence of organisms on the composition of sea-water. In: Hill, M.N. (Ed.), *The Sea*, vol. 2. Wiley, New York, pp. 26–77.
- Scavia, D., Rabalais, N.N., Turner, R.E., Justić, D., Wiseman Jr., W.J., 2003. Predicting the response of Gulf of Mexico hypoxia to variations in Mississippi River nitrogen load. *Limnology and Oceanography* 48, 951–956.
- Scavia, D., Justić, D., Bierman Jr., V.J., 2004. Reducing hypoxia in the Gulf of Mexico: advice from three models. *Estuaries* 27, 419–425.
- Skogen, M.D., Sjøiland, H., Svendsen, E., 2004. Effects of changing nutrient loads to the North Sea. *Journal of Marine Systems* 46, 23–38.
- Steele, J.H., Henderson, E.W., 1992. The role of predation in plankton models. *Journal of Plankton Research* 14, 157–172.
- Strom, S.L., Strom, M.W., 1996. Microplankton growth, grazing, and community structure in the northern Gulf of Mexico. *Marine Ecology Progress Series* 130, 229–240.
- Sutor, M., Dagg, M.J., 2008. The effects of vertical sampling resolution on estimates of plankton biomass and rate calculations in stratified water columns. *Estuarine, Coastal and Shelf Science*, in press, doi:10.1016/j.ecss.2007.11.023.
- Tan, Y.H., Huang, L.M., Chen, Q.C., Huang, X.P., 2004. Seasonal variation in zooplankton composition and grazing impact on phytoplankton standing stock in the Pearl River Estuary, China. *Continental Shelf Research* 24, 1949–1968.
- Walsh, J.J., Penta, B., Dieterle, D.A., Bissett, W.P., 2001. Predictive ecological modeling of harmful algal blooms. *Human and Ecological Risk Assessment* 7, 1369–1383.
- Wawrik, B., Paul, J.H., 2004. Phytoplankton community structure and productivity along the axis of the Mississippi River plume in oligotrophic Gulf of Mexico waters. *Aquatic Microbial Ecology* 35, 185–196.